



Thermal and spectroscopic characterization of gallium-tellurite glasses doped BaF₂ and PbO



Agnieszka Marczevska^{a,*}, Marcin Środa^b, Marek Nocuń^b

^a Institute of Ceramics and Building Materials, Division of Glass and Building Materials in Kraków, Department of Glass Technology, 30-702 Kraków, Lipowa 3, Poland

^b Faculty of Material Science and Ceramics, AGH University of Science and Technology, A. Mickiewicza 30, 30-059 Kraków, Poland

ARTICLE INFO

Article history:

Received 23 January 2017

Received in revised form 14 March 2017

Accepted 15 March 2017

Available online 30 March 2017

Keywords:

Gallium-tellurite glass

Oxyfluoride glass

Thermal stability

Optical properties

BaF₂

PbO

ABSTRACT

The paper studies an influence of Ga₂O₃, PbO and BaF₂ on the thermal stability of tellurite glass and their properties: thermal expansion coefficient, transmittance and refractive index. Three series of gallium-tellurite glass were prepared: I – (100 – x)TeO₂ · xGa₂O₃ where x = 5, 10, 15 and 25 mol%, II – (85 – x)TeO₂ · 15Ga₂O₃ · xBaF₂ where x = 1, 3, 6, 11 mol%, III – (90 – x)TeO₂ · 10Ga₂O₃ · xPbO where x = 0, 5, 10 mol%. It was confirmed that stable gallium-tellurite glass can be produced without applying super-cooling methods in the range 5–15 mol% Ga₂O₃. Ga₂O₃ acts only as a stabilizer of the TeO₂ glassy network when its content not exceed 15 mol%. As shown this effect is connected with the change in crystallization ability of orthorhombic and tetragonal forms of TeO₂. It was found that the latter is preferable when Ga₂O₃ content increases. The increase of the Ga₂O₃ content over 20 mol% induces its spontaneous crystallization. Admixture of BaF₂ and PbO to the Te₂O–Ga₂O₃ glass diminishes a tendency to the glass crystallization. Tellurite glasses with Ga₂O₃, PbO and BaF₂ show good transmittance in the VIS, NIR and MIR up to 5.5 μm. BaF₂ and PbO, unlike Ga₂O₃, decrease the thermal expansion coefficient of tellurite glass. The change in the refractive index due to the admixtures was presented.

© 2017 Elsevier B.V. All rights reserved.

1. Introduction

Gallium-tellurite glass due to the absence of typical glass-forming components is characterized by an increased tendency to crystallization [1]. Despite this, it is interesting optical material with its good transmittance in the IR region up to 6.5 μm. The system Ga₂O₃–TeO₂ has been studied due to the glass forming ability and some properties [2–5]. The tellurite glass is durable and reliable mechanically [6]. The rare earth ions can be easily dissolved in the glass matrix, and the glass is characterized by one of the lowest energy vibration phonons among the oxide glasses [7–8]. With its unique optical properties such as high refractive index and transmittance in the IR range heavy metal tellurite glass is a promising material for applications in nonlinear optics, and in particular for the production of optical fibers and amplifiers [2–3, 6–7, 9–11]. The tellurite glasses can be developed as a material for photonic crystal fibers (PCF) with extremely high non-linearities and wide transmission window [12–14].

Pisarski et al. [15] examined structural and optical properties of Eu³⁺ and Dy³⁺ ions in PbO–Ga₂O₃–XO₂ (X = Te, Ge, Si) glasses using X-ray diffraction, FT-IR and luminescence spectroscopy.

Among the common requirements that must fulfill the glasses, hosts highlight wide transmission ranges from ultraviolet (UV) to mid-infrared (IR), good chemical, mechanical and thermal stabilities, high nonlinear refractive index, and low-energy phonon, which reduce the multiphonon non-radiative probabilities and, consequently, increase the quantum yields. In recent times, a few works are published according to the oxyfluoride tellurite glasses [16–20]. They are devoted to optical and luminescence properties of tellurite glasses. So far, a possibility of the glass-ceramics formation in the oxyfluoride tellurite-based glass for reduction phonon energy of their structure has not been studied. It is known that a decrease of phonon energy of the host for optical active ions enhances their luminescence properties.

The search of novel glasses with low phonon energy, which can provide appropriate matrix for optical active elements is the main reason to conduct this research. Low-phonon glasses Pr³⁺, Tm³⁺, Er³⁺ doped are used as optical amplifiers at a wavelength of 1.3, 1.47 or 1.54 μm, and lasers working at 2 μm. Tellurite glasses are better alternative than fluoride glasses for these purposes in spite of slightly higher phonon energy [21–28].

* Corresponding author.

E-mail addresses: a.marcevska@icimb.pl (A. Marczevska), msroda@agh.edu.pl (M. Środa).

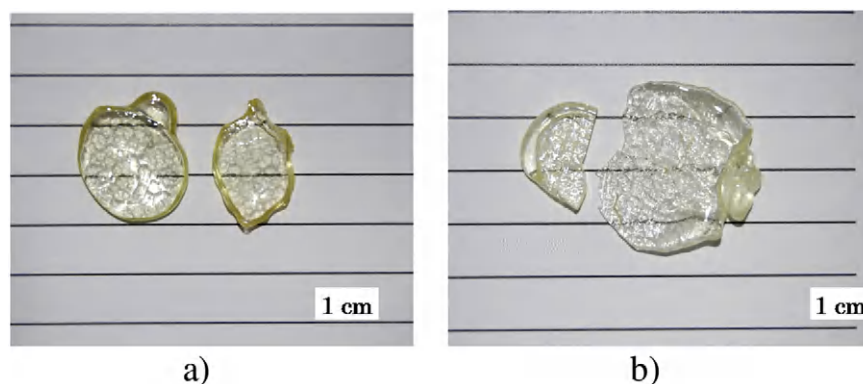
Table 1
Nominal composition of the prepared gallium-tellurite glasses.

Sample	The glass composition [mol%]			
	TeO ₂	Ga ₂ O ₃	BaF ₂	PbO
I series				
95Te5Ga	95	5	–	–
90Te10Ga	90	10	–	–
85Te15Ga	85	15	–	–
75Te25Ga	75	25	–	–
II series				
84Te15Ga1F	84	15	1	–
82Te15Ga3F	82	15	3	–
79Te15Ga6F	79	15	6	–
74Te15Ga11F	74	15	11	–
III series				
85Te10Ga5Pb	85	10	–	5
80Te10Ga10Pb	80	10	–	10

The study of glass area in the TeO₂-Ga₂O₃ and correlation of physic-chemical properties provides a new input to infrared optoelectronic materials. The novel glasses will be applicable to non-linear optical and opto-magnetic devices and lasers. Due to a shift of the long-wave cut-off to 6–7 μm the glasses are promising candidates for optoelectronics and waveguide technology as fibers and gain medium. It is known that tellurite glasses are excellent hosts for the rare earth dopants exhibit the lowest phonon energy among oxide glasses with low tendency to the rare earth clustering.

The main goal of the study was to achieve much lower phonon environment in the low-phonon TeO₂-Ga₂O₃ glass. It can be achieved by fluoride dopants and their nanocrystallization. Such materials can be fabricated based on silicate or aluminosilicate glasses where phonon energy is 1100 cm⁻¹ [29,30].

The goal of the paper is also to show the influence of Ga₂O₃, BaF₂ and PbO on the thermal and spectroscopic properties of tellurite glass as a starting material to develop the optical active glass-ceramic which could be doped the rare earth elements (RE). Tellurite glasses have pho-

**Fig. 1.** The samples of gallium-tellurite glasses: a) 82Te15Ga3F, b) 74Te15Ga11F.**Table 2**
Thermal characteristics of the gallium-tellurite glasses.

Glass no.	T _g /°C	ΔC _p /J/g °C	T _c /°C	ΔH/J/g	ΔT = T _x - T _g /°C	H _r
I series						
95Te5Ga	335 ± 3	0.59 ± 0.02	405 ± 3	104.8 ± 6.8	50	0.36
			417 ± 3	26.2 ± 2.6		
			458 ± 4	1.9 ± 0.4		
			476 ± 4	4.0 ± 0.5		
90Te10Ga	352 ± 2	0.77 ± 0.05	410 ± 5	7.4 ± 0.5	48	0.30
			448 ± 4	96.9 ± 5.6		
85Te15Ga	375 ± 3	0.70 ± 0.04	423 ± 5	4.6 ± 0.6	35	0.25
			459 ± 3	141.0 ± 15.5		
II series						
84Te15Ga1F	372 ± 2	0.71 ± 0.05	424 ± 3	19.1 ± 3.1	31	0.21
			466 ± 2	129.0 ± 9.2		
82Te15Ga3F	369 ± 2	0.51 ± 0.03	435 ± 5	17.6 ± 2.8	42	0.30
			478 ± 3	130.4 ± 10.3		
79Te15Ga6F	367 ± 3	0.47 ± 0.03	447 ± 4	15.8 ± 2.6	55	0.43
			509 ± 3	106.3 ± 8.5		
74Te15Ga11F	366 ± 2	0.65 ± 0.04	433 ± 4	24.7 ± 2.4	46	0.35
			528 ± 5	85.6 ± 7.8		
III series						
85Te10Ga5Pb	348 ± 4	0.80 ± 0.03	402 ± 5	8.8 ± 3.1	38	0.21
			444 ± 5	58.2 ± 5.1		
			486 ± 3	3.4 ± 0.8		
			537 ± 2	43.8 ± 4.6		
80Te10Ga10Pb	352 ± 3	0.86 ± 0.04	396 ± 5	5.6 ± 0.6	30	0.19
			436 ± 4	4.2 ± 0.6		
			471 ± 3	53.3 ± 6.4		

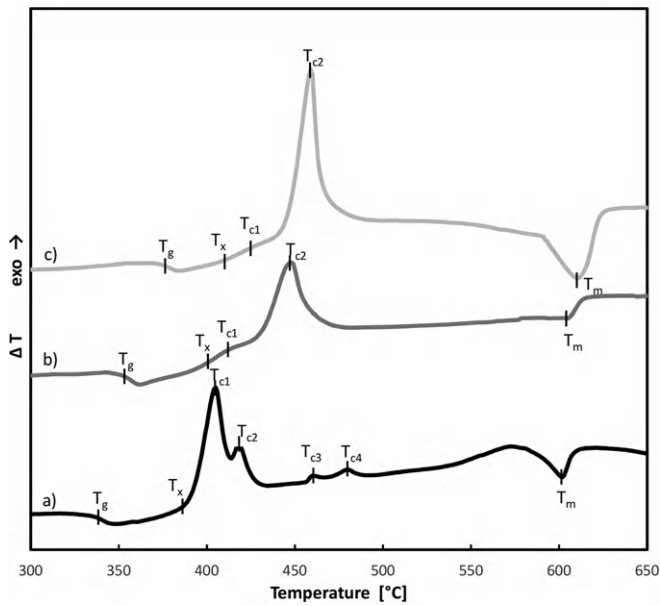


Fig. 2. DTA curves of $\text{TeO}_2\text{-Ga}_2\text{O}_3$ glass with: (a) 5, (b) 10, (c) 15 mol% of Ga_2O_3 .

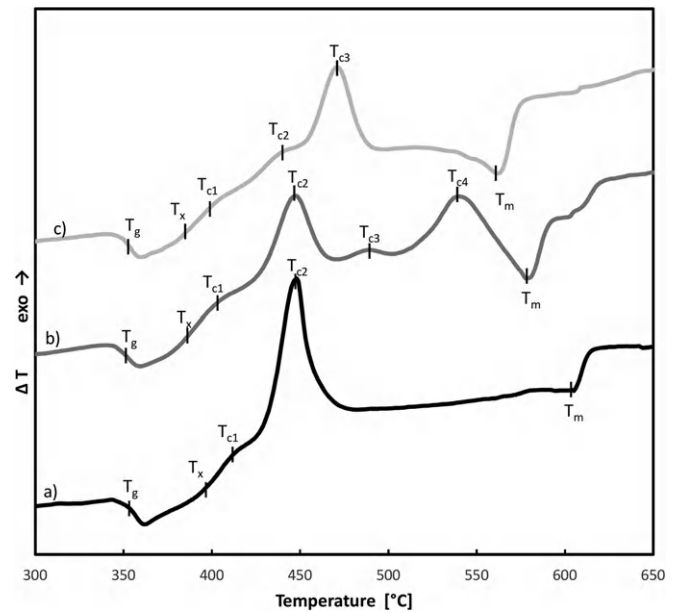


Fig. 4. DTA curves of $\text{TeO}_2\text{-Ga}_2\text{O}_3\text{-PbO}$: (a) 0, (b) 5, (c) 10 mol% of PbO .

non energy ca. 850 cm^{-1} . Fluoride phases have a few times lower values, i.e. $\text{ZrF}_4 - 580\text{ cm}^{-1}$, $\text{LaF}_3 - 350\text{ cm}^{-1}$, $\text{BaF}_2 - 346\text{ cm}^{-1}$, $\text{Pb}_1 - x\text{Cd}_x\text{F}_2 - 235\text{ cm}^{-1}$. Thus, the reason for usage of BaF_2 was to study the possibility to obtain the BaF_2 formation as a host for optical active dopants in the future. The reason for introduction PbO to the tellurite glass was to get knowledge how it influence the thermal stability and transparency of the tellurite glass. Heavy metal oxide PbO enhances optical second harmonic generation output signal due to the high polarizability and it could make a good contribution to optical properties. Controlling the crystallization process in tellurite glasses may increase nonlinear properties by optimizing electronic polarizability and susceptibility with generating nanocrystallites in the glass structure.

2. Experimental

2.1. Synthesis of glass

Three series of gallium-tellurite glass were prepared: I - $(100 - x)\text{TeO}_2 \cdot x\text{Ga}_2\text{O}_3$ where $x = 5, 10, 15$ and 25 mol%, II - $(85 - x)\text{TeO}_2 \cdot 15\text{Ga}_2\text{O}_3 \cdot x\text{BaF}_2$ where $x = 1, 3, 6, 11$ mol%, III - $(90 - x)\text{TeO}_2 \cdot 10\text{Ga}_2\text{O}_3 \cdot x\text{PbO}$ where $x = 5, 10$ mol%. Table 1 presents nominal composition of the batches. The correction of glass composition due to volatility of components was applied based on XRF analysis. The glass was prepared by melting a batch in the platinum crucible in an electric furnace in air atmosphere holding it at the highest temperature of $850\text{--}1000\text{ }^\circ\text{C}$ for 15 min to obtain 0.05 mol (ca. 10 g) of glass. The crucible was covered with a platinum plate during melting. The melt was poured out onto, preheated to $200\text{ }^\circ\text{C}$, a brass plate forming layers $2 \div 3$ mm thick, then annealed at a temperature near the transformation temperature (T_g), ca. $350\text{ }^\circ\text{C}$. The representative samples of casting oxyfluoride glass are shown in Fig. 1.

2.2. Methods of experiments

The ability of the glass to crystallization was determined by DTA/DSC measurements conducted on the Perkin Elmer DTA-7 System operating in heat flux DSC mode for obtaining ΔC_p and ΔH parameters. The 60 mg samples of particle size below 0.05 mm were heated in a platinum crucible at a rate of $10\text{ K}\cdot\text{min}^{-1}$ in dry nitrogen atmosphere up to the temperature of $650\text{ }^\circ\text{C}$. The glass transition temperature T_g was determined from the inflection point on the enthalpy curve; the jump-like changes of the specific heat ΔC_p accompanying the glass transition and the enthalpy of crystallization (ΔH_{cryst}) of the glass were calculated using the 7 Series Perkin Elmer Thermal Analysis Software Library. The ability of glasses to crystallization was measured by the values of the onset crystallization temperature (T_x), the enthalpy of crystallization and the values of the thermal stability parameters of glasses, $\Delta T = T_x - T_g$ and the Hruby parameter, H_r [31]. The representative glasses were selected for further thermal treatment.

The X-ray diffraction patterns (Philips X'Pert Diffractometer with $\text{CuK}\alpha$ radiation) were used to confirm the amorphous nature of glass and determine the products of crystallization after the thermal treatment. In some cases, higher temperature of heat treatment (above the

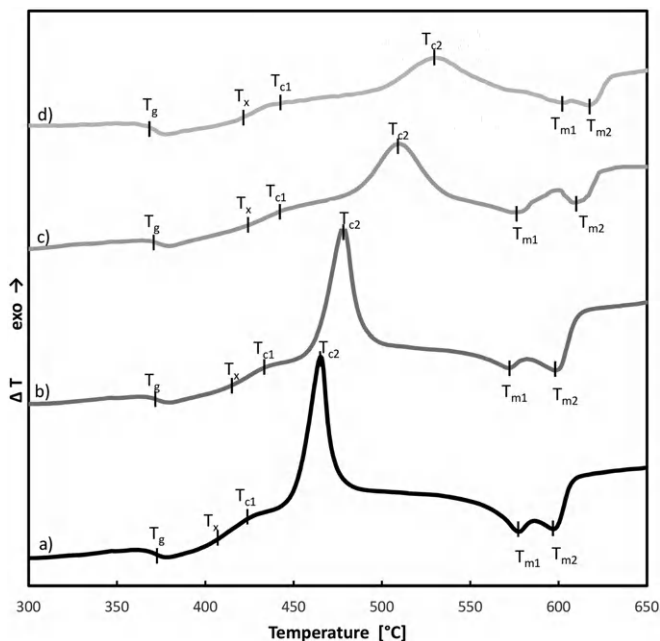


Fig. 3. DTA curves of $\text{TeO}_2\text{-Ga}_2\text{O}_3\text{-BaF}_2$: (a) 1, (b) 3, (c) 6, (d) 11 mol% of BaF_2 .

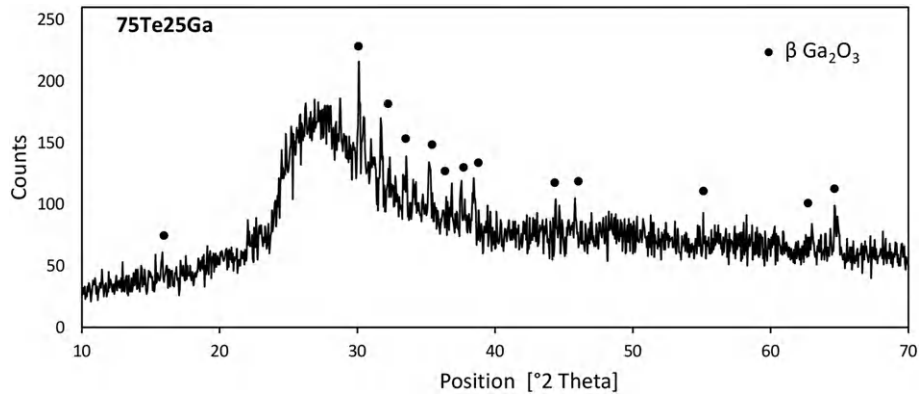


Fig. 5. X-ray diffraction pattern of glass contains 25 mol% Ga₂O₃ with spontaneous crystallization of β-Ga₂O₃ while casting.

crystallization temperature) was applied to get better XRD patterns and due to different conditions of crystallization in DTA analysis and in the furnace during annealing.

The morphology of the samples was studied by SEM/EDS methods (JEOL JSM 5400LV X-ray analyzer 300 Series LINK ISIS). The thermal expansion coefficient of glasses was measured using TMA7 Perkin-Elmer

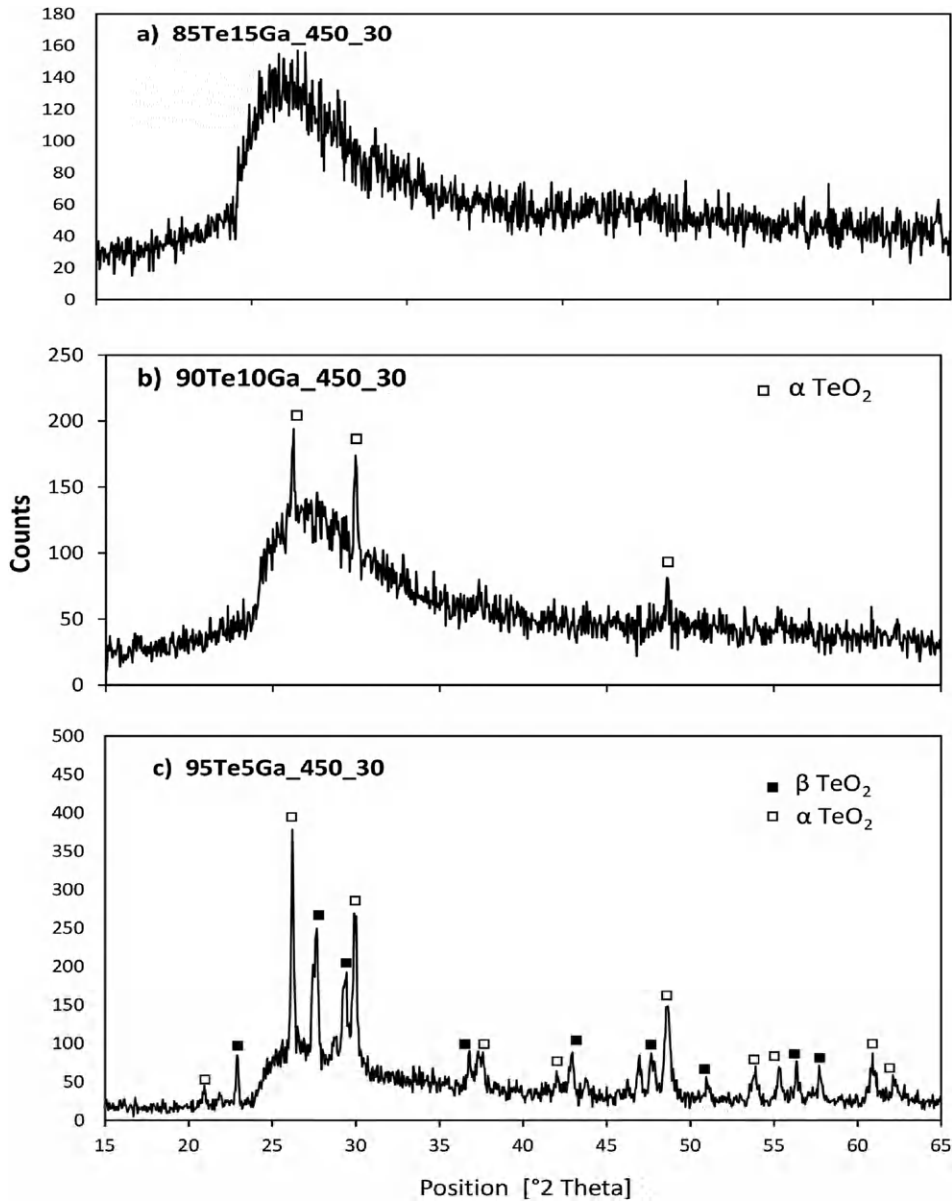


Fig. 6. X-ray diffraction patterns of the heat-treated 85Te15Ga, 90Te10Ga and 95Te5Ga glasses at 450 °C for 30 min.

Table 3
Crystallization of gallium-tellurite glasses.

Class no.	Temperature and the heat treatment time	Products of crystallization
I series		
95Te5Ga	450 °C/30 min	β -TeO ₂ (orthorhombic) and α -TeO ₂ (tetragonal)
	500 °C/30 min	α -TeO ₂
90Te10Ga	450 °C/30 min	α -TeO ₂
85Te15Ga	445 °C/30 min	- ^a
	480 °C/30 min	α -TeO ₂
75Te25Ga	-	Spontaneous crystallization of Ga ₂ O ₃
II series		
84Te15Ga1F	450 °C/30 min	- ^a
	450 °C/24 h	- ^a
82Te15Ga3F	450 °C/30 min	- ^a
	450 °C/24 h	- ^a
79Te15Ga6F	450 °C/30 min	- ^a
	550 °C/30 min	BaF ₂ , Ba ₂ Te ₃ O ₈ , BaTe ₂ O ₅
74Te15Ga11F	450 °C/30 min	No phase
	550 °C/30 min	BaF ₂ , Ba ₂ Te ₃ O ₈ , BaTe ₂ O ₅
III series		
85Te10Ga5Pb	420 °C/30 min	- ^a
	550 °C/30 min	α -TeO ₂ , α -PbO ₂ , PbTeO ₃
80Te10Ga10Pb	420 °C/30 min	- ^a
	480 °C/30 min	α -TeO ₂ , α -PbO ₂

^a No phase detected.

Table 4
Dilatometric analysis of thermal properties.

Sample	Thermal expansion coefficient α [$10^{-6} \text{ } ^\circ\text{C}^{-1}$]		T _{softening} [°C]
	200 °C	300 °C	
I series			
95Te5Ga	13.89	14.06	340
90Te10Ga	13.46	13.94	360
85Te15Ga	12.29	12.75	384
II series			
84Te15Ga1F	12.35	12.86	383
82Te15Ga3F	12.89	13.02	382
79Te15Ga6F	13.08	13.79	380
74Te15Ga11F	13.77	14.26	377
III series			
85Te10Ga5Pb	13.40	13.87	355
80Te10Ga10Pb	14.21	14.99	360

System. An UV/VIS/NIR V-570 Spectrometer from JASCO Company with integrating sphere ILN-472 and Fourier Transform Infrared Spectrometer JASCO FT/IR – 6600 were used to measure transmission from 300 nm to 2.5 μm and from 2.5 μm to 8 μm , respectively. Refraction coefficient was measured by spectroscopy ellipsometer PhE-102 Angstrom Advance.

3. Results

The study shows that in the binary system TeO₂-Ga₂O₃ glass can be obtained in the range 5–20 mol% of Ga₂O₃ with typical rate of casting and thickness of 2–3 mm. For glass with the highest content (25 mol%) of Ga₂O₃ the cloudiness is observed. The BaF₂ and PbO admixtures in the investigated range gave clear and transparent glass.

3.1. DTA/DSC

The glass characterizes the low transformation temperature in the range 335–375 °C. The Ga₂O₃ content affects the increase of T_g (Table 2). A multi-step crystallization which is manifested by four exothermal peaks (two high and two low peaks) on the DTA curve is only observed for glass with 5 mol% Ga₂O₃ (Fig. 2 curve a). The increase of Ga₂O₃ content induces the peaks of crystallization at higher temperature systematically with no trace of the two low peaks. Simultaneously, it leads to vanish the first effect and the next one is observed above 430 °C. The melting temperature shifts higher with Ga₂O₃ content.

The transformation temperature of the II series slowly shifted to lower temperature with the increase of BaF₂ content (Table 2). Simultaneously, temperatures of crystallization increased. Two peaks on the DTA curves for all glasses can be observed (Fig. 3). The first one is broad and the second is being flattened with the increase of BaF₂ what indicates a changes in the kinetic process of the crystallization. Simultaneously, the increase of BaF₂ content induces significant lowering of ΔH for the second effect (Table 2). The endothermic peaks deriving from the melting of the crystallite phases are observed in the range from 560 °C to 630 °C.

The PbO admixture to the gallium-tellurite glass with 10 mol% of Ga₂O₃ (III series) changes significantly the course of crystallization. Two additional exothermal peaks, respectively, at 486 °C and 536 °C can be seen for glass with 5 mol% PbO (Fig. 4, curve b). The further increase of PbO lead to vanish the peak at 536 °C and the main effect is observed at 470 °C (Fig. 4, curve c). Although, there is no change in T_g temperature for the all glasses, the thermal stability, calculated as ΔT and Hruby parameter, decreases when PbO content increases.

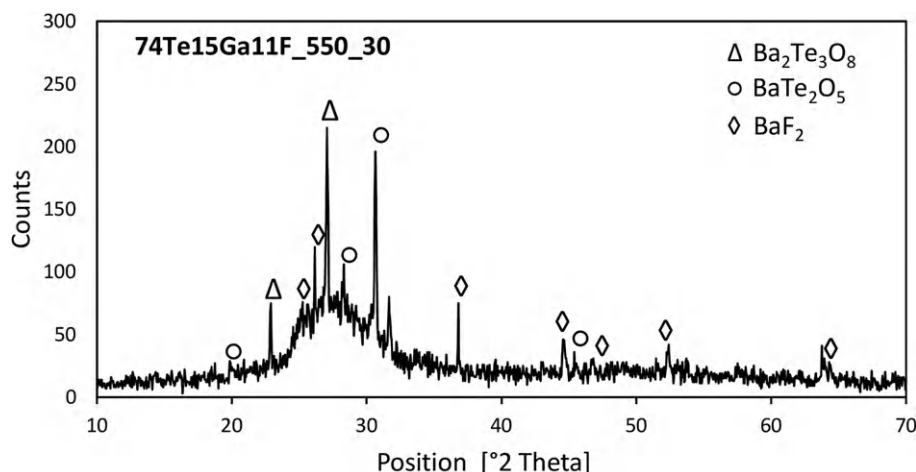


Fig. 7. X-ray diffraction pattern of the heat-treated glass with the highest content of BaF₂ at 550 °C for 30 min.

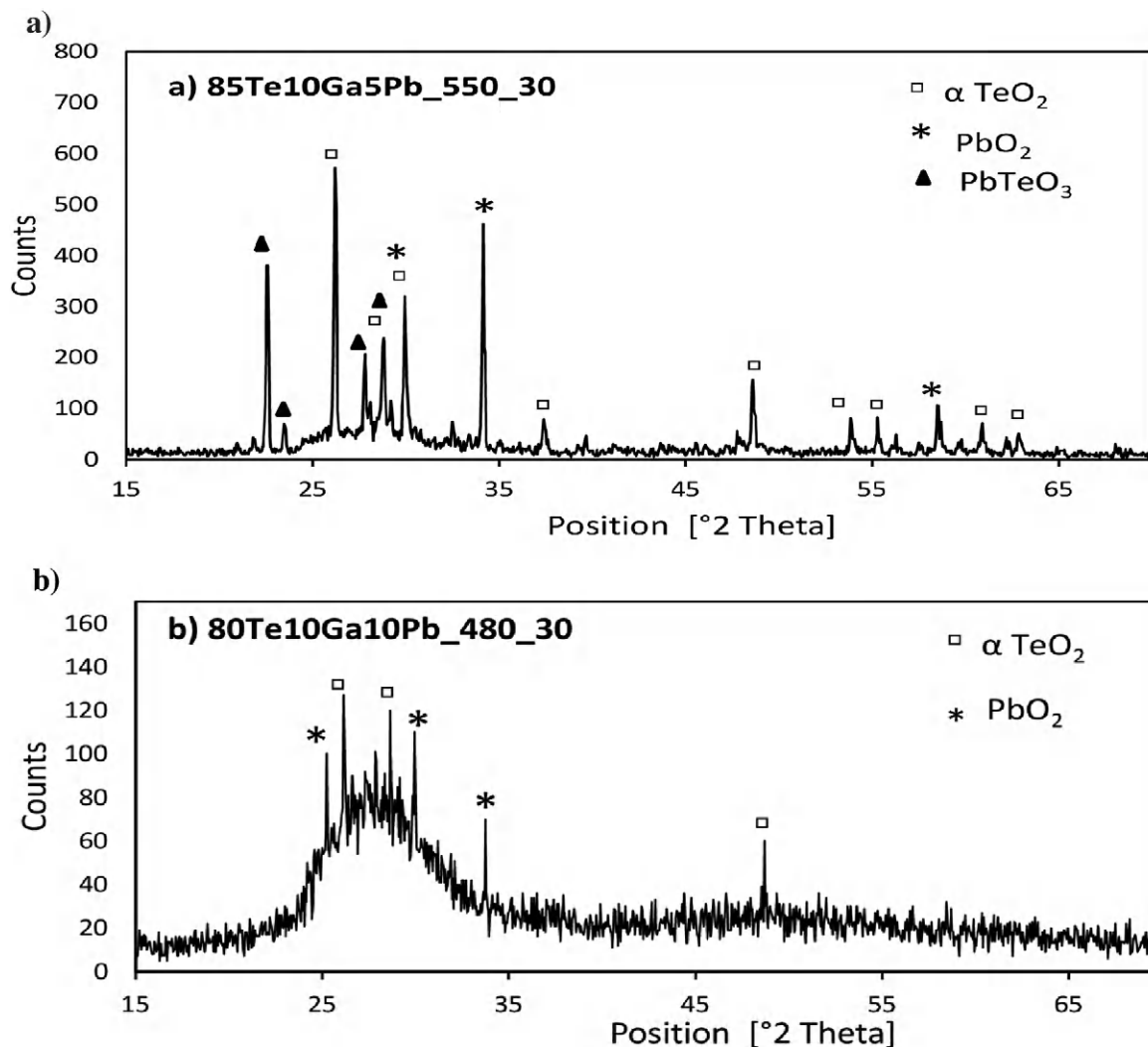


Fig. 8. X-ray diffraction patterns of the glasses with PbO admixtures: a) the heat-treated 85Te10Ga5Pb glass at 550 °C for 30 min, b) heat-treated 80Te10Ga10Pb glass at 480 °C for 30 min.

3.2. XRD analysis

XRD analysis shows that Ga₂O₃ up to 15 mol% stabilized the glassy state. When the glass contains 25 mol% Ga₂O₃ the spontaneous crystallization of β-Ga₂O₃ takes place while the melt is casting (Fig. 5). The heat treatment of the glass leads to formation of orthorhombic β-TeO₂ and tetragonal α-TeO₂ for lower content of Ga₂O₃. The latter is preferable when the network contains more Ga₂O₃ (Fig. 6, Table 3).

Introduction of 1 mol% BaF₂ instead of TeO₂ shifts only the crystallization of α-TeO₂ to the higher temperature. More BaF₂ in the glass changes the course of crystallization. XRD analysis shows formation of Ba₂Te₃O₈ and BaF₂ in place of α-TeO₂ for samples with 6 and 11 mol% of BaF₂.

The admixture of PbO to the TeO₂-Ga₂O₃ glass induces the crystallization of α-TeO₂. XRD analysis of the sample with 5 mol% PbO shows beside TeO₂ the formation of α-PbO₂ at 480 °C and PbTeO₃ at 540 °C, and for sample with 10 mol% PbO only α-TeO₂ and α-PbO₂ was confirmed (Table 3). The results are in line with changes of the peaks intensity observed on the DTA curves (Fig. 8).

3.3. Transmittance properties

The series I shows transmittance from 350 nm to 6.5 μm. Ga₂O₃ increases slightly the transmittance in the visible range of spectrum and

gives no effect in the MIR range (Fig. 9a and 9b). The absorption band at 3–4 μm is due to the presence of OH⁻ groups in the glass structure which was mainly attributable to melting in the air atmosphere. BaF₂ admixture induces slightly reduction of the transmittance in VIS-NIR which is 2% less for content of 11 mol% BaF₂ as compared to the series I. Additionally, the two low absorption bands at 1.40 μm and 1.95 μm become visible with increasing BaF₂ and PbO contents for the series II and III, respectively (Figs. 10a, 11a). The effects may be an indicator of the new bond formation which gives additional overtones or combinations of vibration mode of the structure in the NIR region [32].

BaF₂ characterizes high transmittance in the range from 200 nm to 10 μm with no absorption bands [33]. Thus, the loss of transmittance with increase of BaF₂ content in all range of MIR may result from dispersion and geometry of the equipment without integrating sphere in this range. Nevertheless, the glass shows the absorption edge at ca. 6 μm (Fig. 10b).

PbO admixture reduces transmittance in the VIS range with no significantly influence on IR cut-off (Fig. 11a and b).

3.4. Refractive index measurements

With reference to the curve (a) plotted in Fig. 12 the telluride glasses exhibit a decrease in the refractive index as the Ga₂O₃ and BaF₂ concentration is increased (Fig. 13). Change of *n* for PbO admixtures goes the other way.

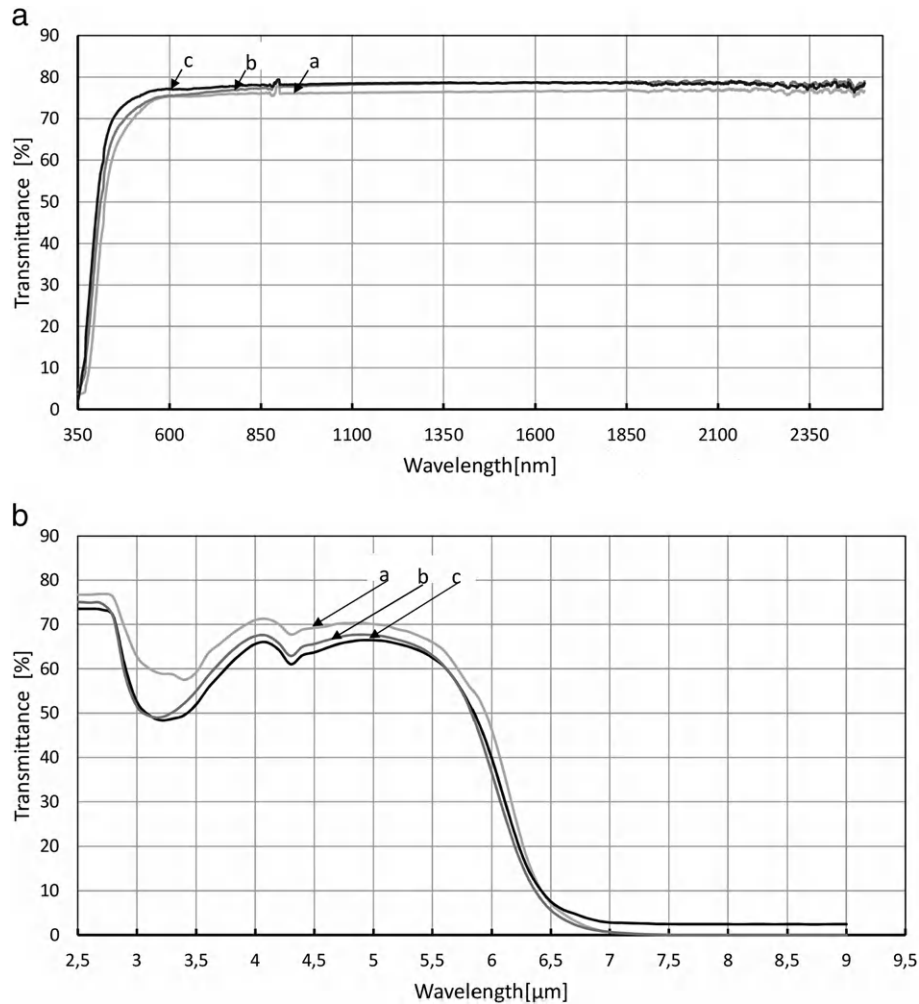


Fig. 9. a. Transmission curves of TeO₂-Ga₂O₃ glass with: (a) 5, (b) 10, (c) 15 mol% of Ga₂O₃ in the range from 300 nm to 2.5 μm. b. Transmission curves of TeO₂-Ga₂O₃ glass with: (a) 5, (b) 10, (c) 15 mol% of Ga₂O₃ in the range from 2.5 to 9 μm.

3.5. Thermal expansion coefficient

The observed trend in the coefficient of thermal expansion is also a significant factor to be considered for the fabrication of composite and optical materials, e.g. fibers. Table 4 shows an influence of Ga₂O₃, BaF₂ and PbO components on the thermal expansion coefficient measured for two ranges of temperature from ambient to 200 °C and to 300 °C, respectively. The temperature of glass softening derived from the expansion curves increases significantly with Ga₂O₃ content (series I). An opposite change are observed for BaF₂ (series II) and PbO (series III) admixtures (Table 4).

4. Discussion

The results show the stable gallium-tellurite glass can be produced by casting in the range from 5 to 20 mol% Ga₂O₃. The tellurite network is made up of trigonal bipyramids [4]. The narrow range of glass formation in the system is due to the restriction of inserting tetrahedra [GaO₄] within the tellurite framework. The consequence of this is spontaneous crystallization of Ga₂O₃ which is observed in the glass with 25 mol% Ga₂O₃ at XRD pattern and SEM analysis (Figs. 5, 15). We show that the optimum content of Ga₂O₃ is 5 ÷ 10 mol% for preparing stable tellurite glass. For this composition the highest thermal stability was achieved (Table 2). The thermal stability of glasses are lower than TeZnNa or TeZnBa glasses which have 100 °C or a little higher but it is

enough to fabricate glass with a normal rate of quenching. The structural units of gallium ions accommodate into tellurite network and inhibit the process of rearrangement and spontaneous crystallization which appears for casting pure tellurite glass. Charton and Armand [5] explain the effect due to unmatching of both structural elements which leads to a considerable distortion of the basic trigonal bipyramids at higher Ga₂O₃ concentration. This structure does not provide a strict local charge neutrality and enough oxygens for Ga³⁺ atoms to form [GaO₄] tetrahedral. We observed it as a reflection of the step change of the specific heat capacity at the range of transformation temperature. The highest value of ΔC_p was obtained for 90Te10Ga glass which shows, simultaneously, the highest thermal stability (the highest values of ΔT, H_f for the series). Moreover, ΔH of α-TeO₂ crystallization is the lowest for the glass. The ΔC_p is the indicator of the configuration entropy caused by increased number of broken bonds (large ΔC_p for fragile liquid [34]) in the course of the glass transformation as a result of rearrangement of glass network induced by gallium admixtures. It is worth to note that Ga₂O₃ influences a change in the course of crystallization, and when its content is high α-TeO₂ appears instead of β-TeO₂ as a product of glass crystallization. It leads to more stable glass what is advantage in the case of PCF formation.

Introduction of BaF₂ into the glass leads to further increase of thermal stability (the increase of ΔT, H_f). Mainly, it is due to a shift of the crystallization peak towards higher temperature. XRD analysis shows the crystallization of Ba₂Te₃O₈ and BaTe₂O₅ instead of α-TeO₂ when the glass contains 6 and 11 mol% BaF₂. Moreover, the XRD analysis

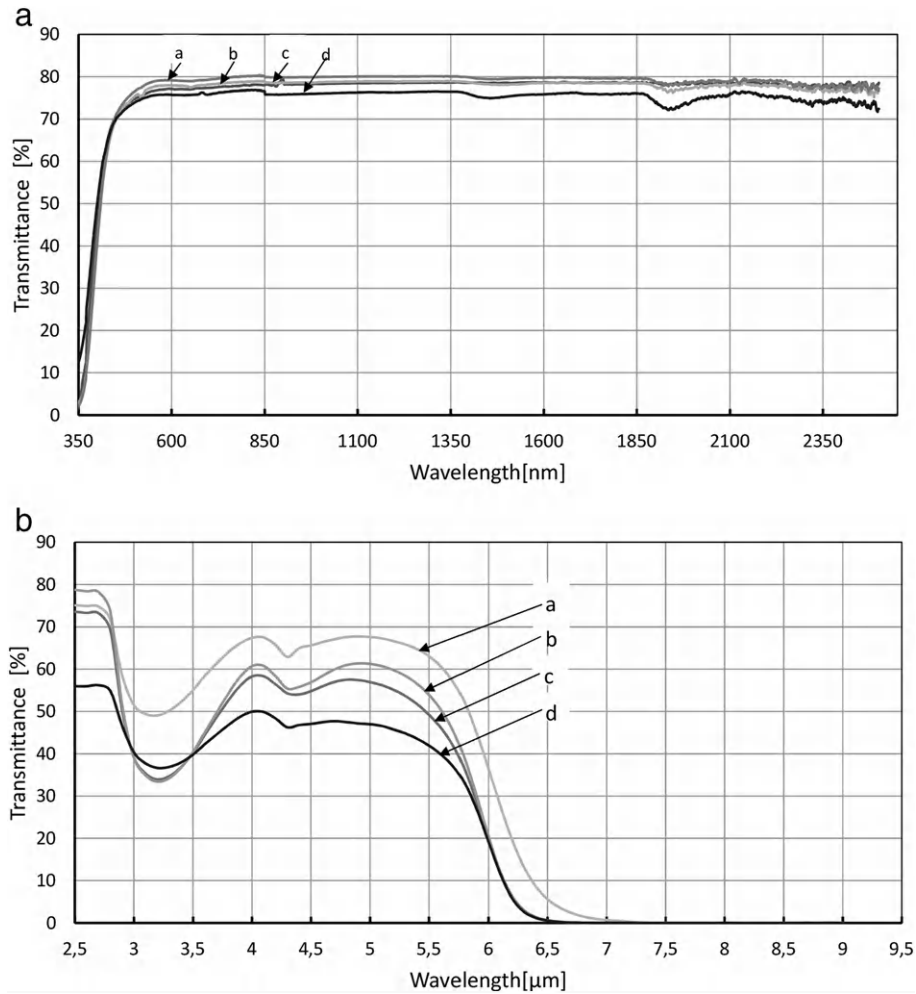


Fig. 10. a. Transmission curves of TeO₂-Ga₂O₃-BaF₂: (a) 0, (b) 1, (c) 3, (d) 11 mol% of BaF₂ in the range from 300 nm to 2.5 μm. b. Transmission curves of TeO₂-Ga₂O₃-BaF₂: (a) 0, (b) 1, (c) 3, (d) 11 mol% of BaF₂ in the range from 2.5 to 9 μm.

confirmed crystallization of the fluoride phase in the glass with the highest content of BaF₂ (Fig. 7). The results show that photonic glass-ceramics with low phonon phase could be produced in the system. The challenge is to get a separation of fluoride from oxide phase crystallization.

Crystallization of fluoride phases has appeared as the first after exceeding T_g in oxyfluoride glasses with silicate network [35]. Thus, a shift of the small but visible exothermal effect on DTA curve (Fig. 3d) to lower temperature for 74Te15Ga11F sample may be just associated with minor crystallization of BaF₂. On the other hand, increase of Ba²⁺ ions leads to significant reduction of ΔH . Barium plays the role of modifiers in the silicate glass and induces breaking of the Si-O-Si bridges [31, 36]. Our results shows that Ba²⁺ ions stabilize the tellurite framework. It can be achieved by increase of flexibility of Te-polyhedra in the network or/and by impeding arrangement of the Te-network caused by Ba-octahedra. Barium attenuates the crystallization of TeO₂. Instead of that the BaTe₂O₅ and Ba₂Te₃O₈ are formed at higher temperature.

The refractive index of tellurite glasses exhibit very high values. Our values of n are similar to the results reported by others authors for tellurite glasses [37].

The structure and chemical bonding state in RO-TeO₂ glasses have been studied extensively. It is well recognized that the structure of TeO₂-based glasses consists of [TeO₄] trigonal bipyramids and [TeO₃] trigonal pyramids and the fraction of [TeO₃] structural units with non-bridging oxygen increases with increasing RO content [38–39]. The decrease in the refractive index for Ga₂O₃ and BaF₂ admixtures can be understood in terms of the conversion of the highly polarizable [TeO₄] to

the less polarizable [TeO₃] and the decrease of the network polymerization. Fargin et al. [39] and Suehara et al. [40] indicate that the polarizability of the [TeO₃] unit is substantially less than that of the [TeO₄] unit. Furthermore, an increase of modifier concentration is at the expense of the concentration of TeO₂. Ga and Ba possess lower polarizabilities than Te [37,41–42], thus one would expect the network polarizability and consequently the refractive indices to decrease, as is observed. On the other hand, the formation of [TeO₄] structural units are favourable when a modifier transition metal is added to the glass [43–44]. PbO shows the similar effect with the increase in refractive index (Fig. 14).

For an usage of glasses as optical fibers, the thermal expansion of the cladding and core must be match with a slightly higher value of α for the latter [44]. It is generally accepted that a pair of materials should have $\Delta\alpha < 5 \cdot 10^{-6} \text{ }^\circ\text{C}^{-1}$ [45]. For the all glass series the variation of the thermal expansion coefficient fulfills the restriction. The variation of α is $2.24 \cdot 10^{-6} \text{ }^\circ\text{C}^{-1}$ over the entire range of modifiers' concentrations.

5. Conclusions

The effect of admixture Ga₂O₃, BaF₂ and PbO on the formation of tellurite glasses was studied. It was showed that stable gallium-tellurite glass can be melt in the range 5–15 mol% Ga₂O₃. In this range the Ga₂O₃ induces an increase of the thermal stability which was calculated as the ΔT and Hruby criterion. It was shown that the orthorhombic form of TeO₂ declines and the tetragonal one is preferable when Ga₂O₃ content increases.

When PbO is incorporated into gallium-tellurite glass the lowering tendency to the TeO₂ crystallization is observed (lower ΔH).

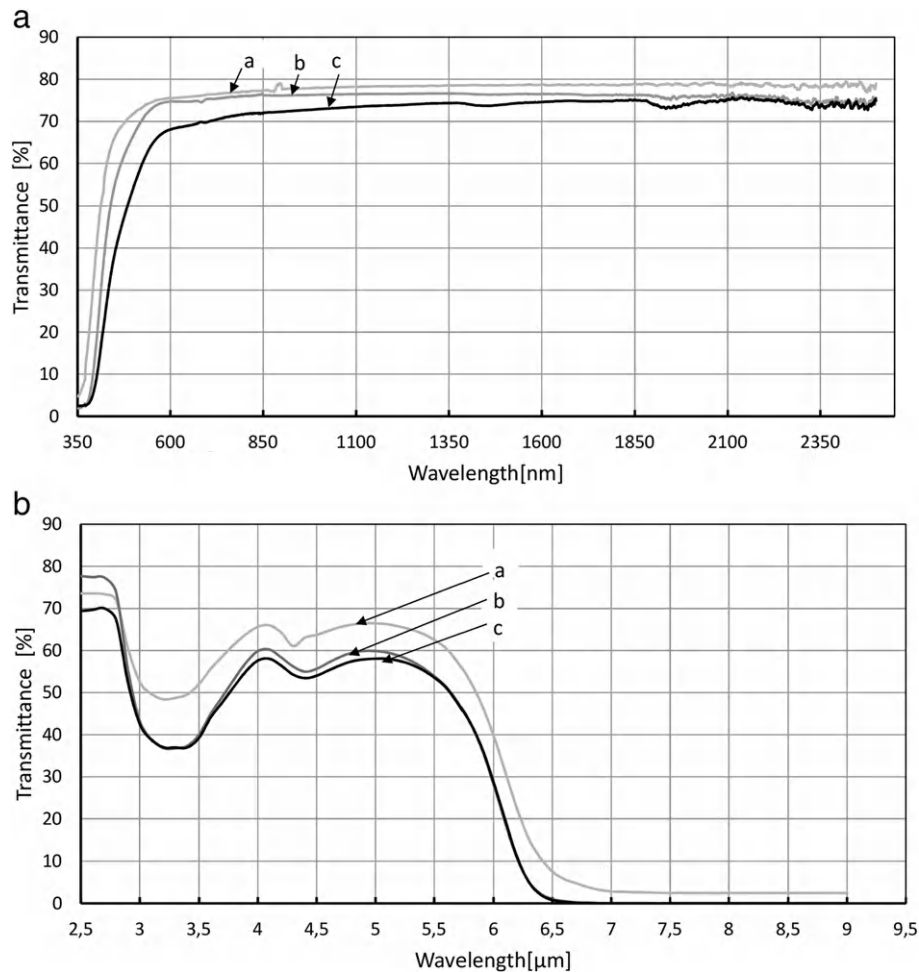


Fig. 11. a. Transmission curves of TeO₂-Ga₂O₃-PbO: (a) 0, (b) 5, (c) 10 mol% of PbO in the range from 300 nm to 2.5 μm. b. Transmission curves of TeO₂-Ga₂O₃-PbO: (a) 0, (b) 5, (c) 10 mol% of PbO in the range from 2.5 to 9 μm.

Admixture of BaF₂ to the Te₂O-Ga₂O₃ glass increases the thermal stability. The formation of low phonon phase BaF₂ was confirmed after heat treatment of the gallium-tellurite glass with 11 mol% of BaF₂ in the glass composition. It gives opportunity to develop the oxyfluoride-tellurite glass-ceramics as up-conversion optical materials with low phonon host working in the near and mid-infrared regions.

PbO and BaF₂ retain the good transparency of tellurite glass in the IR region.

Acknowledgments

This work was supported by the statutory funds of Institute of Ceramics and Building Materials (No. 3NS16T17) Division of Glass and

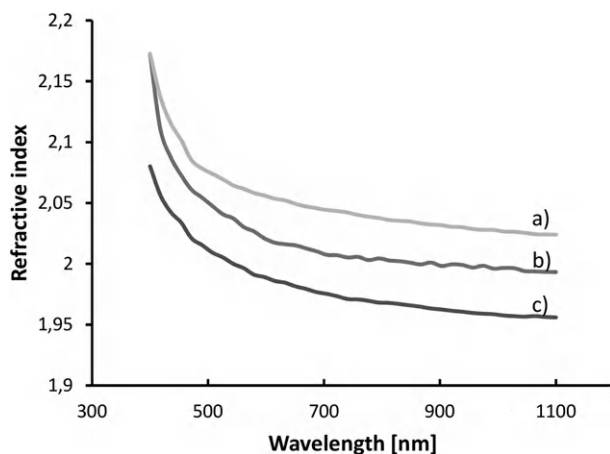


Fig. 12. Dispersion of refractive index of TeO₂-Ga₂O₃ glass samples with: (a) 5, (b) 10, (c) 15 mol% of Ga₂O₃ obtained from ellipsometric measurements.

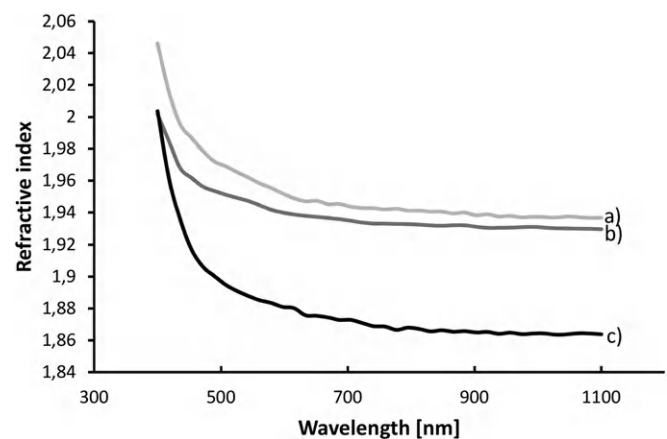


Fig. 13. Dispersion of refractive index TeO₂-Ga₂O₃-BaF₂ glass samples with: (a) 1, (b) 3, (c) 11 mol% of BaF₂ obtained from ellipsometric measurements.

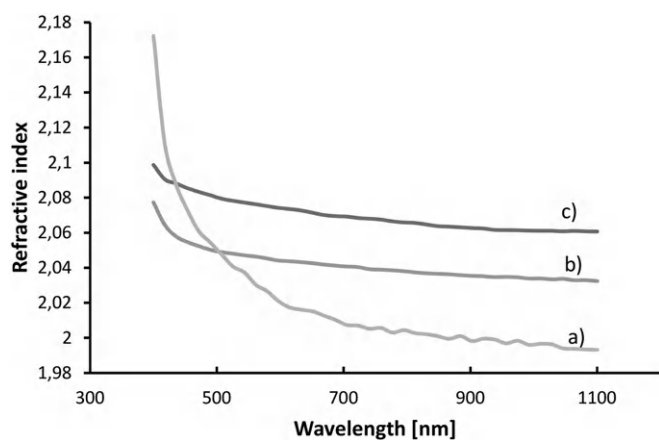
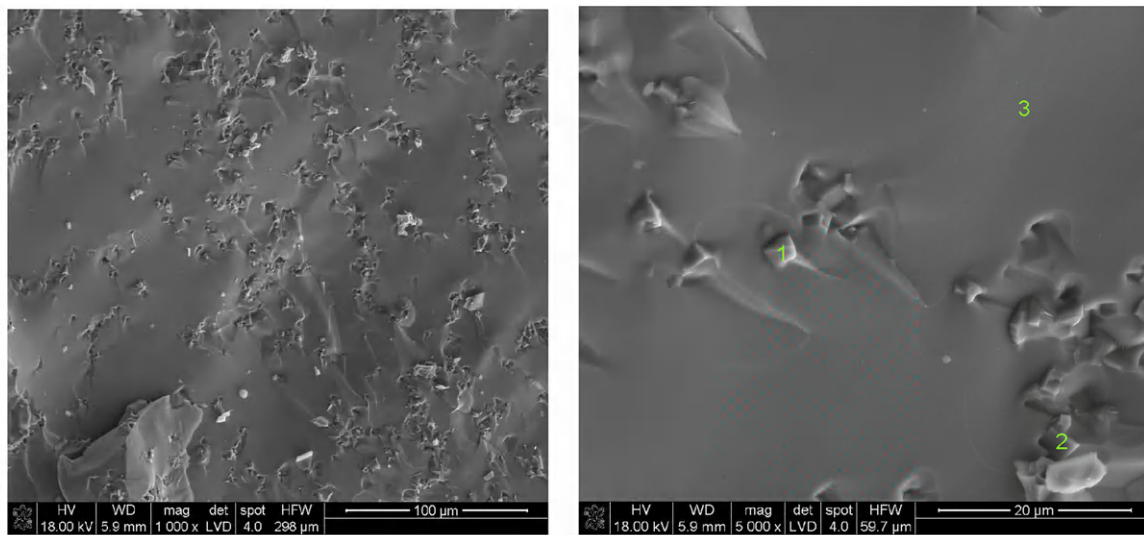


Fig. 14. Dispersion of refractive index $\text{TeO}_2\text{-Ga}_2\text{O}_3\text{-PbO}$ glass samples with: (a) 0, (b) 5, (c) 10 mol% of PbO glass obtained from ellipsometric measurements.

Building Materials in Krakow and AGH University of Science and Technology Department of Materials Science and Ceramics AGH number WIMiC No 11.11.160.365 in 2017.

References

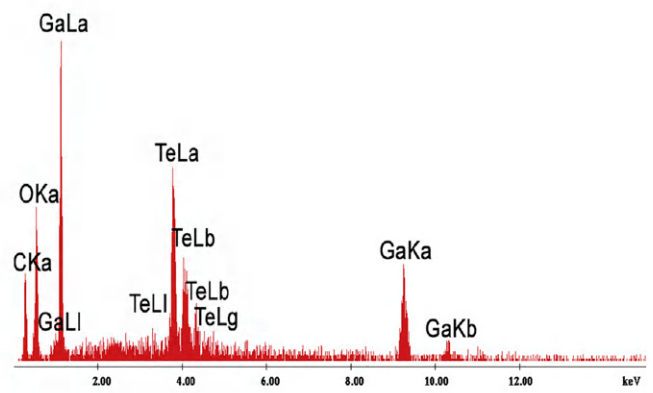
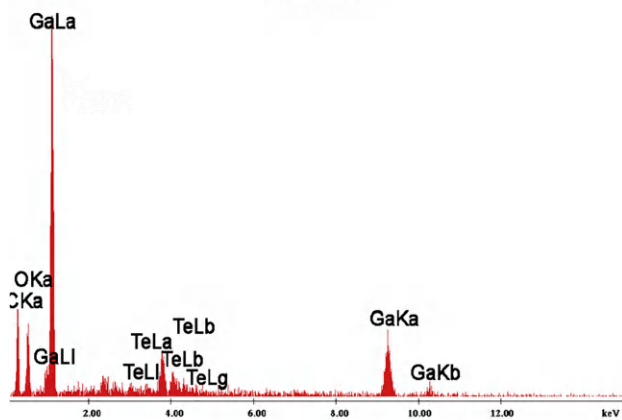
- [1] N.S. Tagiara, D. Palles, E.D. Simandiras, V. Psycharis, A. Kyritsis, E.I. Kamitsos, *J. Non-Cryst. Solids* 457 (2017) 116–125.
- [2] A. Jha, B. Richards, G. Jose, T. Teddy-Fernandez, P. Joshi, X. Jiang, J. Lousteau, *Prog. Mater. Sci.* 57 (2012) 1426–1491.
- [3] H. Lin, K. Liu, E.Y.B. Pun, T.C. Ma, X. Peng, Q.D. An, J.Y. Yu, S.B. Jiang, *Chem. Phys. Lett.* 398 (2004) 146–150.
- [4] V. Petkov, O. Stachs, Th. Gerber, D. Ilieva, Y. Dimitriev, *J. Non-Cryst. Solids* 248 (1999) 65–74.
- [5] P. Charton, P. Armand, *J. Non-Cryst. Solids* 333 (2004) 307–315.
- [6] R. Stępień, R. Buczyński, D. Pysz, I. Kujawa, A. Filipkowski, M. Mirkowska, R. Diduszek, *J. Non-Cryst. Solids* 357 (2011) 873–883.
- [7] H.X. Yang, H. Lin, L. Lin, Y.Y. Zhang, B. Zhai, E.Y.B. Pun, *J. Alloys Compd.* 453 (2008) 493–498.
- [8] H. Lin, S. Tanabe, L. Lin, Y.Y. Hou, K. Liu, D.L. Yang, T.C. Ma, J.Y. Yu, E.Y.B. Pun, *J. Lumin.* 124 (2007) 167–172.
- [9] A. Ghosh, R. Debnath, *Opt. Mater.* 31 (2009) 604–608.
- [10] I. Kujawa, R. Kasztelaniec, R. Stępień, M. Klimczak, J. Cimek, A.J. Waddie, M.R. Taghizadeh, R. Buczyński, *Opt. Laser Technol.* 55 (2014) 11–17.
- [11] S.Q. Man, E.Y.B. Pun, P.S. Chung, *Opt. Commun.* 168 (1999) 369–373.
- [12] Z. Duana, H.T. Tonga, M. Liaoa, T. Chenga, M. Erwanb, Takenobu, Y.O. Suzukia, *Opt. Mater.* 35 (2013) 2473–2479.
- [13] T.L. Cheng, D.H. Deng, X.J. Xue, T. Suzuki, Y. Ohishi, *Appl. Phys. Lett.* 104 (2014) 1.
- [14] T.H. Tuan, L. Zhang, T. Suzuki, Y. Ohishi, *Opt. Commun.* 381 (2016) 282–285.
- [15] W.A. Pisarski, J. Pisarska, L. Żur, T. Goryczka, *Opt. Mater.* 35 (2013) 1051–1056.
- [16] L.N. Ignatieva, N.N. Savchenko, Yu.V. Marchenko, I.G. Maslennikova, G.A. Zverev, V.K. Goncharuk, *J. Non-Cryst. Solids* 450 (2016) 103–108.
- [17] A. Wagh, V. Petwal, J. Dwivedi, V. Upadhyaya, Y. Raviprakash, S.D. Kamath, *Radiat. Phys. Chem.* 126 (2016) 37–48.
- [18] E.A. Lalla, U.R. Rodríguez-Mendoza, A.D. Lozano-Gorrín, A. Sanz-Arranz, F. Rull, V. Lavín, *Opt. Mater.* 51 (2016) 35–41.
- [19] A. Miguel, M.A. Arriandiaga, R. Morea, J. Fernandez, J. Gonzalo, R. Balda, *J. Lumin.* 158 (2015) 142–148.
- [20] A. Miguel, R. Morea, M.A. Arriandiaga, M. Hernandez, F.J. Ferrer, C. Domingo, J.M. Fernandez-Navarro, J. Gonzalo, J. Fernandez, R. Balda, *J. Eur. Ceram. Soc.* 34 (2014) 3959–3968.
- [21] B. Tang, Ch. Wu, J. Li, Y. Fan, H. Hu, L. Zhang, *J. Non-Cryst. Solids* 355 (2009) 2006–2009.
- [22] E.F. Chillce, I.O. Mazali, O.L. Alves, L.C. Barbosa, *Opt. Mater.* 33 (2011) 389–396.
- [23] A. Maaoui, F. Ben Slimen, M. Haouari, A. Bulou, B. Boulard, H. Ben Ouada, *J. Alloys Compd.* 682 (2016) 115–123.
- [24] U.R. Rodríguez-Mendoza, E.A. Lalla, J.M. Caceres, F. Rivera-Lopez, S.F. Leon-Luis, V. Lavín, *J. Lumin.* 131 (2011) 1239–1248.
- [25] G. Gao, G. Wang, Ch. Yu, J. Zhang, L. Hu, *J. Lumin.* 129 (2009) 1042–1047.
- [26] F. Yang, Ch. Liu, D. Wei, Y. Chen, J. Lu, S. Yang, *Opt. Mater.* 36 (2014) 1040–1043.
- [27] J. Fan, B. Tang, D. Wu, Y. Fan, R. Li, J. Li, D. Chen, L. Calveza, X. Zhang, L. Zhang, *J. Non-Cryst. Solids* 357 (2011) 1106–1109.
- [28] Ch. Cheng, Y. Yu, F. Zhang, H. Zhang, J. Qiu, *J. Non-Cryst. Solids* 406 (2014) 1–4.
- [29] M. Środa, Z. Olejniczak, *J. Non-Cryst. Solids* 357 (2011) 1696–1700.
- [30] S.H. Lee, S. Bae, Y.G. Choi, W.J. Chung, *J. Non-Cryst. Solids* 431 (2016) 126–129.
- [31] J. Zarzycki, *Glasses and the Vitreous State*, Cambridge University Press, 1991.
- [32] L. Bokobza, *J. Near Infrared Spectrosc.* 6 (1998) 3.
- [33] <http://eksmaoptics.com/optical-components/uv-and-ir-optics/barium-fluoride-baf2-windows/> 2017.
- [34] A.K. Varshneya, *Fundamentals of Inorganic Glasses*, Society of Glass Technology, 2006.
- [35] M. Środa, I. Wacławska, L. Stoch, M. Reben, *J. Therm. Anal. Calorim.* 77 (2004) 193–200.
- [36] M. Rai, G. Mountjoy, *J. Non-Cryst. Solids* 401 (2014) 159–163.
- [37] T. Sekiya, N. Mochida, A. Ohtsuka, M. Tonokawa, *J. Non-Cryst. Solids* 168 (1994) 106–114.
- [38] Y. Himei, Y. Miura, T. Nanba, A. Osaka, *J. Non-Cryst. Solids* 177 (1994) 164–169.
- [39] E. Fargin, A. Berthreau, T. Cardinal, G. Le Flem, L. Ducasse, L. Canioni, P. Segonds, L. Sarger, A. Ducasse, *J. Non-Cryst. Solids* 203 (1996) 96–101.
- [40] S. Suehara, P. Thomas, A.P. Mirgorodsky, T. Merle-Mejean, J.C. Champarnaud-Mesjard, T. Aizawa, S. Hishita, S. Todoroki, T. Konishi, S. Inoue, *Phys. Rev. B* 70 (2004) 205121/1–205121/7.
- [41] W.A. Capanema, K. Yukimitu, J.C.S. Moraes, F.A. Santos, M.S. Figueiredo, S.M. Sidel, V.C.S. Reynoso, O.A. Sakai, A.N. Medina, *Opt. Mater.* 33 (2011) 1569–1572.
- [42] S. Manning, H. Ebendorff-Heidepriem, T.M. Monro, *Opt. Mater. Express* 2 (2) (2012) 140–152.
- [43] J.C. Sabadel, P. Armand, D. Cachau Herreillat, P. Baldeck, O. Doctot, A. Ibanez, E. Philippot, *J. Solid State Chem.* 132 (1997) 411–419.
- [44] M.D. O'Donnell, K. Richardson, R. Stolen, A.B. Seddon, D. Furniss, V.K. Tikhomirov, C. Rivero, M. Ramme, R. Stegeman, G. Stegeman, M. Couzi, T. Cardinal, *J. Am. Ceram. Soc.* 90 (2007) 1448–1457.
- [45] J. Wang, J.R. Lincoln, W.S. Brocklesby, R.S. Deol, C.J. Mackechnie, A. Pearson, A.C. Tropper, D.C. Hanna, D.N. Payne, *J. Appl. Phys.* 73 (1993) 8066–8075.



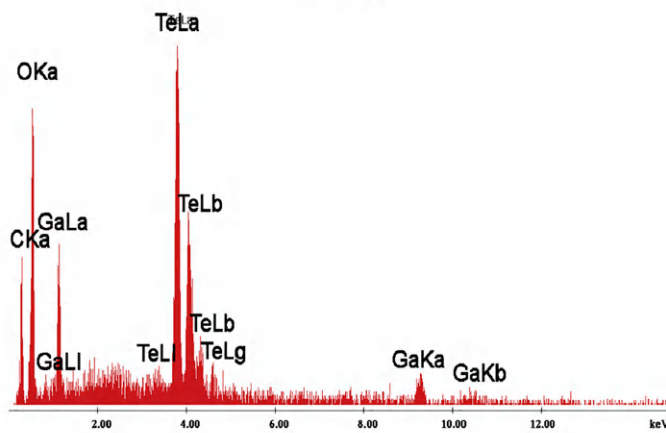
(a)

Point 1

Point 2



Point 3



(b)

Fig. 15. (a) SEM micrograph of the 75Te25Ga sample and (b) EDS analysis for the points.